To appear in the Astronomical Journal

Proper-Motion Measurements with the VLA. II. Observations of Twenty-eight Pulsars

W. F. Brisken,[1] A. S. Fruchter,[2] W. M. Goss,[1] R. S. Herrnstein,[3] and S. E. Thorsett[4]

ABSTRACT

Using the Very Large Array, we have measured the proper motions of twenty-eight radio pulsars. On average, the pulsars studied are fainter and more distant than those studied in earlier work, reducing the selection biases inherent in surveys restricted to the Solar neighborhood. The typical measurement precision achieved is a few milliarcseconds per year, corresponding to a few tens of kilometers per second for a pulsar a kiloparsec away. While our results compare well with higher-precision measurements done using very-long baseline interferometry, we find that several earlier proper motion surveys appear to have reported overly optimistic measurement uncertainties, most likely because of a failure to fully account for ionospheric effects. We discuss difficulties inherent in estimating pulsar velocities from proper motions given poorly constrained pulsar distances. Our observations favor a distribution with 20% of pulsars in a low velocity component ($\sigma_{1D} = 99$ km s^{-1}) and 80% in a high velocity component ($\sigma_{1D} = 294$ km s^{-1}). Furthermore, our sample is consistent with a scale height of pulsar birthplaces comparable to the scale height of the massive stars that are their presumed progenitors. No evidence is found in our data for a significant population of young pulsars born far from the plane. We find that estimates of pulsar ages based on kinematics agree well with the canonical spin-down age estimate, but agreement is improved if braking indexes are drawn from a Gaussian distribution centered at n=3 with width 0.8.

Subject headings: pulsars: general—stars: neutron—stars: kinematics—astrometry

[1]National Radio Astronomy Observatory, P.O. Box 0, Socorro, New Mexico 87801 wbrisken@nrao.edu; mgoss@nrao.edu

[2]Space Telescope Science Institute, 3700 San Martin Dr., Baltimore, MD 21218 fruchter@stsci.edu

[3]Columbia Astrophysics Laboratory, Mail Code 5247, 500 West 120th St. New York, NY 10027

[4]Department of Astronomy and Astrophysics, University of California, 1156 High St., Santa Cruz, CA 95064 thorsett@ucolick.org

1. Introduction

Radio pulsars are a high velocity stellar population, with typical speeds of hundreds of kilometers per second, induced by asymmetries in their birth supernova events or through breakup of progenitor binary systems. Although most pulsars are probably born very near the plane of the Galaxy, they can move to a kiloparsec or more above the plane in a few million years. Most proper motion studies have been limited to the bright, nearby pulsars in the Solar neighborhood, and therefore miss a significant fraction of the highest velocity stars. This bias must be considered when attempting to estimate the birth velocity distribution from the observations. The initial velocity distribution contains valuable information about supernova symmetry and the progenitor binary properties and is an essential input parameter to binary population synthesis studies and for calculations of the neutron star retention rate in globular clusters. Considerable effort has therefore been expended in trying to understand the effects of survey incompleteness on the observed pulsar velocity distribution.

An alternative approach is to reduce the bias by expanding the volume of the Galaxy in which pulsar proper motions are measured. In 1992, we set out to do that with a long-term study of a sample of relatively distant pulsars, using the NRAO[5] Very Large Array (VLA) telescope facility. In McGary et al. (2001, Paper I), we briefly described the motivation for this work and our target selection criteria, and we described our observational method, which we review in §2. In this report, we present proper motion measurements for twenty-eight pulsars (§3). In a few cases, previous measurements with lower precision are available from other surveys, allowing us to test the reliability of these surveys.

Velocity estimates require combining our results with distance estimates. In §4, we discuss the importance of distance uncertainties in estimating pulsar velocities and we estimate the distances of the pulsars in our sample. Finally, in §5 we present some discussion of the implications of this work. We calculate the relatively bias free velocity distribution using a sample of 36 pulsars with reliable proper motion measurements. Additionally for the young pulsars of this sample we compute the probability distribution function (PDF) for kinetic age and hence compute the fraction of young pulsars that appear to be falling toward the Galactic plane.

---

[5]The National Radio Astronomy Observatory is a facility of the National Science Foundation operated under cooperative agreement by Associated Universities, Inc.

2. Observations

The observations and data analysis techniques have been discussed in detail in Paper I, and are briefly reviewed here.

We observed 28 pulsars during observing campaigns at the VLA centered at epochs 1992.96, 1994.23, 1995.52, 1998.32, and 1999.47. Most observations were made in the A-array, with a typical beam size of 1.3 arcsec. A small number of observations were made during the reconfiguration to B-array in 1998, with beam sizes up to 4 arcsec. Only the two circular polarization products, RR and LL, were simultaneously correlated; the linear polarization products were not retained as that would have reduced the available bandwidth without increasing the sensitivity. A 25 MHz wide band at 1452 MHz was divided into 15 frequency channels to reduce bandwidth smearing over a wide field, which allowed identification of multiple in-beam astrometric reference sources for each pulsar. Typical image noise levels ranged between 0.1 and 0.2 mJy beam^{-1}. In many cases, the VLA correlator was "gated" for one polarization, to accumulate data only during the on-pulse portion of the pulsar period. By eliminating the accumulation of noise during the off-pulse portion, the signal-to-noise ratio was improved by up to a factor of five. This, together with the high sensitivity of the VLA, allowed observation of fainter—and more distant—sources than in previous studies. The second polarization was ungated to maximize sensitivity to the reference sources. We performed tests to verify that the astrometry was not affected by the gating, comparing the position measurements from the two polarizations. Agreement to 5 mas or better was achieved for the brightest reference sources; statistical uncertainties dominated for the weaker sources. For the brighter pulsars the gate was not used and the two polarizations were summed. A summary of the pulsar observations can be found in Table 1.

Earlier VLA observations made at $\lambda \sim 21$ cm were also available for four of our target pulsars. We reanalyzed the archival raw data. Most of these data were observed for previous position or proper motion surveys (in particular, Fomalont et al. 1992 & 1997). These observations proved valuable as they roughly doubled the time span of some of the position measurements. Including these data was not entirely straight forward, however. Because these earlier observations were made with a 50 MHz bandwith divided into fifteen channels, the effect of bandwidth smearing is about twice as great. The positional uncertainties of reference sources far from the field center were increased in the radial direction to properly account for this. The observation frequency for these additional observations was 1385 MHz, rather than 1452 MHz, resulting in a 5% larger beam, 10% larger ionospheric effects, and possibly slightly different structure in the reference sources. None of these effects is great enough to affect the results. In the end, addition of the archival data did not appreciably

change the proper motion results (typical improvement was 20%). This is mainly due to less time on source than for the new observations and to the lack of gating. Although an earlier observation of B1237+25 was made, it was not included in our analysis. These archival observations did provide additional confidence that the proper motions values reported here are correct. Additionally, B2106+44 was observed as a test target with the VLA and the Pie Town VLBA antenna in 2001 and these data were included in our analysis.

Flux density and bandpass calibration were obtained from observations of 3C48, 3C147, or 3C286. Observations of each pulsar were alternated with observations of a nearby ($< 20^\circ$) phase calibrator. Phase and amplitude solutions were interpolated between calibrator observations and applied as complex gain corrections to the pulsar visibilities. Self calibration was performed in all cases. Self calibration is an iterative process that leads to self-consistent calibration resulting in a maximized signal-to-noise ratio. For gated measurements, the self-calibration solutions from one polarization were copied to the other polarization. Uncertainties in the phase calibrator position and differential ionospheric and tropospheric phases limit the absolute pulsar position measurements to about 0.1 arcseconds.

Analysis was done in the AIPS software package. The task UVFIX was run to recover the correct (u, v, w) values and timestamps for the source. This is needed for high-precision astrometry since the VLA correlator does not include special relativistic corrections for diurnal and annual abberation and the timestamps reported are for the start of integration, not the midpoint (see Fomalont et al. 1992 for discussion on this topic). Images were made using the CLEAN algorithm. Self-calibration was used to improve estimates of the phase and amplitude errors. Self-calibration can reduce the accuracy of absolute position measurement, however the relative astrometry, used here to measure the motions of the pulsars, is improved due to the increase in sensitivity. JMFIT was used to fit a Gaussian brightness distribution to the pulsar and the compact reference sources producing position measurements and their uncertainties. An error-ellipse for each position measurement was computed in order to correctly account for covariances in the x and y position uncertainties. See Paper I for more details on our use of UVFIX and JMFIT.

3. Proper Motions and Uncertainties

Pulsar positions and proper motions were determined through a χ^2 minimization that simultaneously fit for the positions of each of the reference source and the pulsar, the proper motion of the pulsar, and a small residual systematic coordinate deformations relating each epoch's coordinate system to that of the first epoch. The magnitude of these coordinate deformations were strongly dependent on the source declination, suggesting differential re-

fraction through the ionosphere and troposphere (see Paper I) as a cause. The transformation was parameterized as a six parameter linear transformation. In the cases where the fit residuals were high, the reference sources were investigated. Those that showed proper motion significant at the 2σ level or very high fit residuals were removed. In all cases, removal of between zero and three reference sources from the fit produced residuals that were consistent with the measurement uncertainties. These sources likely experienced structure changes, such as ejection of material into a jet or relative brightness changes of components, that are unresolved with the VLA but none-the-less produce astrometic shifts. For pulsars with four or more epochs, uncertainties in the proper motions could also be estimated using bootstrap Monte-Carlo techniques (Press et al. 1986). Where this was possible, the agreement between the methods was excellent, and we believe that the uncertainties derived from the least squares fitting are accurate, even for the less-sampled sources. We believe that our final errors are dominated by the Gaussian measurement uncertainties and that the final error bars are very nearly the Gaussian 1σ widths. The astrometric results are summarized in Table 2. See Paper I for additional details on the fitting and Monte-Carlo methods. It should be noted that no strong covariances between the proper motion and other fit parameters were observed.

For all but three of the pulsars observed, these new results were either the first or the most accurate proper motion measurements. Two of the exceptions, B0919+06 (Chatterjee et al. 2001) and B1237+25 (Brisken et al. 2002) were observed using the Very Long Baseline Array (VLBA) using proven techniques. Single-epoch VLBA position measurements of these pulsars were accurate to about 0.2 mas. The third, B1534+12, is a stable millisecond pulsar with a very accurate timing proper motion (Stairs et al. 1998). Except for a single 2σ deviation, in the measurement of μ_α for B1237+25, our new proper motion measurements were all within one standard deviation of these more accurate results. These results are consistent with Gaussian statistics.

The new proper motions are compared against previously determined proper motions in Table 3 with differences between the previous and our proper motion components expressed in units of the combined-in-quadrature uncertainties.

Because of their high precision, our results are valuable for testing the reliability of the published error bars of previous interferometric measurements. We have thirteen sources that have also been observed by other studies: five in a one-baseline experiment at Jodrell Bank (Lyne et al. 1982), four in a two-baseline experiment at Jodrell Bank (Harrison et al. 1993), and four in a previous program at the VLA (Fomalont et al. 1997). Except for two results that deviated by more than 3σ, the proper motions in right ascension agree quite well, whereas only five of thirteen pulsars agree to better than 2σ in declination, suggesting

an underestimate of the declination proper motion uncertainties in previous measurements. It is possible that the ionosphere and unaccounted structures of sources near the pulsars in the Jodrell Bank proper motions contributed to additional uncertainty. The ionosphere will tend to increase uncertainties in the declination more than the right ascension since most observations are scheduled near transit, the time when the gradient in the ionosphere's strength is largely in declination. Our use of 1452 MHz reduced the ionosphere's effect by a factor of 12.7 over the previous 408 MHz observations at Jodrell Bank.

4. Distance uncertainties

If a pulsar's distance is known, the observed proper motion can be reduced to a physical transverse velocity; hence distance measurements are very important for kinematic studies of pulsars.

A pulsar's distance can be estimated by combining the line-of-sight electron column density, or dispersion measure (DM), with a model of the Galactic electron distribution. Normally, uncertainty in the DM can be ignored, so the precision of this method depends only on the Galactic electron model. For the last decade, the standard model has been that of Taylor and Cordes (1993; hereafter T&C). [6] Except for a few pulsars associated with objects at known distance, such as globular clusters, annual parallax is the only model-independent method to obtain the distance to a pulsar. Because most parallax measurements were made after the development of the T&C model, and were not used in the development of the model, they provide a uniquely powerful test of the model. A comparison was made by Brisken et al. (2002), who found that the model could predict the DM to a given distance to about 40% accuracy. Although this fractional precision was determined from pulsars within about a kiloparsec of the Sun, we have assumed the same precision at greater distances.

Understanding the statistics of distance measurements is important when modeling populations, since incorrect uncertainty estimates can bias results. For example, a sample with excessively large estimates of uncertainty will be biased towards greater distance. Further, in almost all cases, the non-uniform model distribution of electrons produces significantly non-Gaussian distance uncertainties. At the extreme are pulsars with DMs comparable to the model's total electron column density in a particular distance. In these cases the pulsars' distances are unbounded by the DM measurement. Examples of distance uncertainties from both dispersion and parallax measurements are shown in Fig. 1.

[6] Although new models (Gómez et al. 2001 and Cordes & Lazio 2002) have recently been introduced, we continue to use the T&C model for consistency with earlier results.

5. Discussion

Given a sample of pulsars with well-measured proper motions, we can address a number of questions about pulsar kinematics. However, even with 28 pulsars our sample is small. We considered adding earlier proper motion measurements, most with poorer precision, but as described above we have found that the error bars assigned to these measurements are not well understood. We were, however, able to supplement our sample with six additional sources younger than 20 Myr, whose proper motions were reliably measured by Brisken et al. (2002), using VLBI. Table 4 contains a list of these pulsars and some of their properties.

5.1. The birth velocity distribution

Extraction of the pulsar birth velocity distribution from a selected sample of proper motions of middle-aged pulsars with poorly known distances is a task riddled with bias, uncertainty, and confusion. Nevertheless, the result is crucial to such questions as the fraction of pulsars that escape the Solar neighborhood (and in turn the local birthrate, the supernova rate, the rate of enrichment of the interstellar medium, and the minimum mass for a star to undergo a supernova explosion), the fraction of newborn neutron stars retained in globular clusters, and the dynamics of supernova collapse. Hence we follow many other authors in tackling the question, while cautioning that much work remains and our results should not be overinterpreted. In particular, although our sample was chosen specifically to reduce sample bias, we believe the sample size is still too small to effectively measure and remove the residual bias that undoubtedly remains.

Sample bias entered the problem initially in the pulsar discovery surveys. Searches are obviously dependent on the pulsar flux density and hence on luminosity and distance, but they are more subtly biased even for pulsars with the same luminosity and distance. For example, the sensitivity depends (in a generally complex way) on DM, galactic coordinates, declination, pulse period, and pulse shape. All of these quantities may be correlated with velocity. For example, if proper motion and spin axis are correlated, then pulsars that have moved far from the galactic plane will be detected with less efficiency, or if luminosity is related to velocity then the resultant velocity distribution will be biased. Age is almost certainly correlated with distance from the galactic plane, meaning searches targeting the Galactic plane will inherently bias the sample of known pulsars. Pulsars moving quickly away from the Galactic plane spend less time within their detection radius. As pulsars get farther away their motion tends toward purely radial. Additionally, the Galactic gravitational potential significantly accelerates a pulsar after a period of about 10^7 years.

Bias gets compounded when proper motion samples are chosen. It is most straightforward to measure proper motions of brighter objects, which tend to be even closer than the typical known pulsars. Since the highest speed pulsars leave the local sample volume more quickly than the slower pulsars the resultant mean velocity is lowered.

Ideally, proper motion studies would sample a very large volume and be limited to pulsars that are young enough to minimize loss from the sample or deceleration in the Galactic potential. Discovery and measurement limitations and the small number of very young pulsars make such an ideal study impossible, leading many authors (Hansen & Phinney 1997; Arzoumanian et al. 2002; Lorimer et al. 1997) to attempt to measure or otherwise estimate the biases and correct the sample. We have taken a different approach, trying to reduce the size of the biases with more accurate measurements that allowed a larger sample volume. However, the tradeoff is that, in our judgment, the resulting sample size is too small to allow sophisticated analysis of the remaining bias.

We have addressed the problem of Galactic acceleration, and further reduced the problem of sample incompleteness, by limiting our analysis to the single velocity component perpendicular to the line of sight and parallel to the Galactic plane: v_l is the product of distance, D, and the corresponding component of proper motion, μ_l. In our analysis, we first tabulate for each pulsar $P(v_l)$, the PDF for v_l. This calculation is complicated by the distance dependence on the Galactic rotation correction, $\Delta_{v_l}(D)$, and assumes the form

$$P(v_l) = \int_0^\infty dD \int_{-\infty}^\infty d\mu_l \, \delta\left(v_l - (D\,\mu_l - \Delta_{v_l}(D))\right) P(D)\, P(\mu_l). \tag{1}$$

In practice, this is integrated numerically from tabulated $P(D)$ and $P(\mu_l)$ PDFs.

With this set of PDFs different velocity models can be tested. The likelihood, L, that a model $P(v_l;\vec{m})$ with model parameters $\vec{m}$, explains the measurements, $P_i(v_l)$ is:

$$L = \prod_i \int dv_l \, P_i(v_l)\, P(v_l;\vec{m}). \tag{2}$$

Comparing different model forms, especially those with different numbers of parameters, is difficult to do in an unbiased manner, we will use the same model form that was used by Arzoumanian et al. (2002) (hereafter ACC). This model contained three parameters describing the widths of two zero-centered Gaussian distributions, and the fraction of pulsars in the first:

$$P(v_l;\sigma_1,\sigma_2,w_1) = \frac{w_1}{\sqrt{2\pi\sigma_1^2}} \exp(-v_l^2/2\sigma_1^2) + \frac{1-w_1}{\sqrt{2\pi\sigma_2^2}} \exp(-v_l^2/2\sigma_2^2). \tag{3}$$

This is the analog of Eqn. 1 in ACC for use with a single component of the velocity, hence the velocity dispersions, σ_{v_i} in ACC is a factor of $\sqrt{3}$ larger than the corresponding value,

σ_i, in Eqn. 3. Maximizing the likelihood (Eqn. 2) results in a best fit with $\sigma_1 = 99$ km s^{-1}, $\sigma_2 = 294$ km s^{-1}, and $w_1 = 0.20$. These model parameters are preferred to those of ACC ($\sigma_1 = 52$ km s^{-1}, $\sigma_2 = 289$ km s^{-1}, $w_1 = 0.4$) by an odds ratio of 7.7 (see ACC). A plot of the resultant 1-dimensional velocity PDFs for both our fit and that of ACC is shown in Fig. 2.

5.2. Pulsar birth locations

Based on the low scale height of massive O and B stars, it is conventionally assumed that most or all neutron stars recently formed in the Milky Way were born very near the Galactic plane. However, Harrison et al. (1993) found that 17% of the young pulsars in their sample were falling towards the plane, perhaps indicating a second group of pulsar progenitors with large scale height. As pulsars born out of the plane only have a 50% chance of being born with a velocity pointing towards the plane, and as many of these will rapidly pass through the plane (a pulsar born at 150 pc above the plane moving towards the plane with 150 km s^{-1} only takes one million years to reach the plane) and then appear to be moving away from the plane, the work of Harrison et al., if confirmed, would imply a very large high birth-height population. One original motivation for our work was, therefore, to determine better the size of the population of infalling pulsars.

Old pulsars may be moving towards the plane not because they were born with velocity vectors pointing towards the plane, but rather because the Galactic potential has over course time caused their infall. Pulsars older than about 20 Myr will have undergone a significant fraction of an oscillation about the Galactic plane, and therefore could potentially contaminate any study of the birth heights of pulsars.

A geometric method to estimate a pulsar's age is to divide the angular distance traversed during the pulsar's lifetime by its proper motion. Again, for this age estimate to be reliable, its true age must be less than about 10 Myr. This kinetic age, $\tau_{\rm kin}$, is given as

$$\tau_{\rm kin} = \frac{D \sin b - z_0}{\mu_b D \cos b + v_r \sin b}, \tag{4}$$

where D is the pulsar's distance, z_0 is its birth height, and v_r is the pulsar's radial velocity. The birth height and radial velocity cannot be measured so an initial distribution must be assumed. A birth height distribution with scale height $\sigma_{z_0} = 150$ pc is assumed. The pulsar birth height distribution is not well known. The distribution chosen here is chosen as a compromise between a modeled pulsar birth height of 175 pc (Stollman, 1987), and the supernova scale height, ~ 100 pc (based on Green, 2001). Note that both of these estimates are made without pulsar kinematics statistics. It should be noted that this scale

height is consistent with that derived by the simulations of ACC ($z_0 = 160 \pm 40$ pc). The radial velocity distribution is a 1-D component of the full velocity, analogous to what was measured in § 5.1. The radial velocity requires a distance dependent correction, $\Delta v_r(D)$, due to differential Galactic rotation and solar motion. Although we are aware that various projection effects will cause the radial velocity distribution to be different than the velocity distribution measured above, we will use that distribution. The PDF for kinetic age can then be computed:

$$\begin{aligned} P(\tau_{\rm kin}) &= \int dz_0 \int dD \int dv_r \int d\mu_b \, \delta \left(\tau_{\rm kin} - \frac{D \sin(b) - z_0}{\mu_b D \cos(b) + (v_r + \Delta v_r(D)) \sin(b)} \right) \times \\ & P_{z_0}(z_0|\sigma_{z_0}) P_D(D|DM) P_{v_r}(v_r) P_{\mu_b}(\mu_b|\mu_{b,\rm meas}, \sigma_{\mu_b}). \end{aligned} \tag{5}$$

A negative kinetic age would imply that the pulsar is falling toward the plane. The probability that a pulsar is falling towards the plane, $P_{\rm fall}$ can be computed:

$$P_{\rm fall} = \int_{-\infty}^{0} d\tau_{\rm kin} \; P_{\tau_{\rm kin}}(\tau_{\rm kin}). \tag{6}$$

From a sample of pulsars with calculated $P_{\rm fall}$ we wish to calculate the probability $P(f)$ that a fraction f of young pulsars are falling based on the set of $P_{\rm fall}$ values for pulsars with ages less than 20 Myr. Although significant acceleration could occur within 20 Myr, less than one quarter of an orbit would have completed by this time, which maintains the sign of $\tau_{\rm kin}$

$$\begin{aligned} P(f) &= P(f|\{P_{\rm fall,i}\}) \\ &\propto P(\{P_{\rm fall,i}\}|f) P_{\rm prior}(f), \end{aligned} \tag{7}$$

where Bayes theorem was again used. A flat prior PDF, $P_{\rm prior}(f)$, is assumed. Since all of the data are independent this can be expanded as a product of single pulsar probabilities:

$$P(f) \propto \prod_i P(P_{\rm fall,i}|f), \tag{8}$$

where the conditional PDF has the form

$$P(P_{\rm fall}|f) = 2P_{\rm fall} f + 2(1 - P_{\rm fall})(1 - f). \tag{9}$$

Note that integrating this over $0 \leq P_{\rm fall} \leq 1$ yields 1, regardless of the value of f.

We used a sample of 26 pulsars (20 from this study, and 6 from Brisken et al. (2002)) with characteristic age less than 20 Myr. $P(f)$ was computed on a grid of values between 0 and 1, and is plotted in Fig. 3. We conclude that, with 68% confidence, fewer than 6% of young pulsars are falling towards the plane (fewer than 11% at 95% confidence). Contrary to earlier studies, we find that a population of pulsars with large birth height is not required.

5.3. Timing ages and braking indexes

Timing properties can be used to estimate the age of a pulsar. The basic assumption that a pulsar's spin frequency, $\nu = 1/P$, evolves via power-law decay, $\dot{\nu} \propto -\nu^n$, leads to an age,

$$\tau = \frac{P}{(n-1)\dot{P}} \left[1 - \left(\frac{P_0}{P} \right)^{n-1} \right], \tag{10}$$

where P and $\dot{P}$ are the pulsar's spin period and spin period time derivative, respectively. The pulsar's initial spin period, P_0, is generally assumed to be much smaller than its current period. However, the 39 ms pulsar B1951+32, associated with supernova remnant CTB80, has $P_0 = 27 \pm 6$ ms (Migliazzo et al. 2002). Likewise, the 143 ms pulsar J0538+2817 must have a $P_0 \gtrsim 130$ ms based on the likely association with S147 (Romani & Ng 2003). These examples suggest that $P_0 \ll P$ is not strictly true. The braking index n depends on the dominant torque acting on the pulsar. It is believed that electromagnetic dipole radiation, with $n = 3$, dominates for most pulsars. The characteristic age, $\tau_{\rm char}$, is thus defined by Eqn. 10 with this value of n and with the assumption that $P_0 \ll P$:

$$\tau_{\rm char} = \frac{P}{2\dot{P}}. \tag{11}$$

This value is generally used to estimate pulsar ages.

A pulsar's kinetic age PDF can be used to determine its braking index PDF. Since the initial periods of none of the pulsars in the sample are known, a scale invarient PDF for the initial period was used with a lower cutoff of 5 ms. The smaller of the pulsar's period or 200 ms was used as the upper cutoff. The results are not very sensitive to these cutoffs. It is implicitly assumed that the braking index of a pulsar remains constant throughout its life. The desired PDF can be expressed as

$$P_n(n) = \int dP_0 \int d\tau \, \delta(n - n(P, \dot{P}, P_0, \tau)) \, P_\tau(\tau) \, P_{P_0}(P_0), \tag{12}$$

where $n(P, \dot{P}, P_0, \tau)$ is Eqn. 10 reexpressed for the value of n, and τ is the true age of the pulsar. Here we use the kinetic age for the true age and its PDF, $P_\tau(\tau)$ is derived in Eqn. 5. The braking index PDFs for 21 pulsars (16 from this paper and 5 from Brisken et al., 2002) with $\tau_{\rm char} < 10$ Myr and $|b| > 1^\circ$ are shown schematically in Fig. 4.

The distribution of pulsar braking indexes can be derived from a set of braking index PDFs. In this analysis we assume the form of the braking index distribution is Gaussian with two model parameters, the mean, n_0, and the width, σ_n. The distributions are truncated below $n = 1$. Flat priors are used for n_0 and σ_n. This analysis proceeded analogously to

Eqn. 2. The model parameters yielding the greatest likelihood are $n_0 = 2.98$ and $\sigma_n = 0.82$. This width is prefered over the most likely zero-width distribution, that with $n_0 = 2.64$, by an odds ratio of 403. This strongly suggests that there is an intrinsic width to the distribution of braking indexes, as expected given the handful of direct measurements of the braking indexes of young pulsars (see Table 5). It is not certain that these values are representative of all pulsars. The magnitude of the width suggests that the characteristic age, $\tau_{\rm char}$, can only be trusted to about 40%.

SET is supported by NSF grant AST-0098343. The graduate work of WFB was partially funded by an NSF graduate student fellowship. Special thanks go to Mike Nolta for the creation of the Biggles plotting package, which was used exclusively in this publication. We thank the anonymous referee who provided useful feedback.

REFERENCES

Arzoumanian, Z., Chernoff, D. F., & Cordes, J. M. 2002, ApJ, 568, 289

Brisken, W. F., Benson, J. M., Goss, W. M., & Thorsett, S. E. 2002, ApJ, 571, 906

Camilo, F. M., Kaspi, V. M., Lyne, A. G., Manchester, R. N., Bell, J. F., D'Amico, N., McKay, N. P. F., & Crawford, F. 2000, ApJ, 541, 367

Chatterjee, S., Cordes, J. M., Lazio, T. J. W., Goss, W. M., Fomalont, E. B., & Benson, J. M. 2001, ApJ, 550, 287

Cordes, J. M. & Lazio, T. J. W. 2002, ApJ, submitted, http://xxx.lanl.gov/abs/astro-ph/0207156

Fomalont, E. B., Goss, W. M., Lyne, A. G., Manchester, R. N., & Justtanont, K. 1992, MNRAS, 258, 497

Fomalont, E. B., Goss, W. M., Manchester, R. N., & Lyne, A. G. 1997, MNRAS, 286, 81

Gómez, G. C., Benjamin, R. A., & Cox, D. P. 2001, Astron. J., 122, 908

Gouiffes, C., Finley, J. P., & Ögelman, H. 1992, ApJ, 394, 581

Green D. A. 2001, supernova catalog, `http://www.mrao.cam.ac.uk/surveys/snrs/`

Hansen, B. & Phinney, E. S. 1997, MNRAS, 291, 569

Harrison, P. A., Lyne, A. G., & Anderson, B. 1993, MNRAS, 261, 113

Kaspi, V. M., Taylor, J. H., & Ryba, M. 1994, ApJ, 428, 713

Lorimer, D. R., Bailes, M., & Harrison, P. A. 1997, MNRAS, 289, 592

Lyne, A. G., Anderson, B., & Salter, M. J. 1982, MNRAS, 201, 503

Lyne, A. G., Pritchard, R. S., Graham-Smith, F., & Camilo, F. 1996, Nature, 381, 497

Lyne, A. G., Pritchard, R. S., & Graham-Smith, F. 1993, MNRAS, 265, 1003

McGary, R. S., Brisken, W. F., Fruchter, A. S., Goss, W. M., & Thorsett, S. E. 2001, Astron. J., 121, 1192 (referenced as Paper I)

Migliazzo, J. M., Gaensler, B. M., Backer, D. C., Stappers, B. W., Van der Swaluw, E., & Strom, R. G. 2002, ApJ, 567, L141

Press, W. H., Flannery, B. P., Teukolsky, S. A., & Vetterling, W. T. 1986, Numerical Recipes: The Art of Scientific Computing (Cambridge: Cambridge University Press)

Romani, R. W., & Ng, C.-Y. 2003, ApJ, 585, L41

Stairs, I. H., Arzoumanian, Z., Camilo, F., Lyne, A. G., Nice, D. J., Taylor, J. H., Thorsett, S. E., & Wolszczan, A. 1998, ApJ, 505, 352

Stollman, G. M. 1987, A&A, 178, 43

Taylor, J. H. & Cordes, J. M. 1993, ApJ, 411, 674

Taylor, J. H., Manchester, R. N., Lyne, A. G., & Camilo, F. 1995, unpublished (available at `ftp://pulsar.princeton.edu/pub/catalog`).

Urama, J. O. 2002, MNRAS, 330, 58

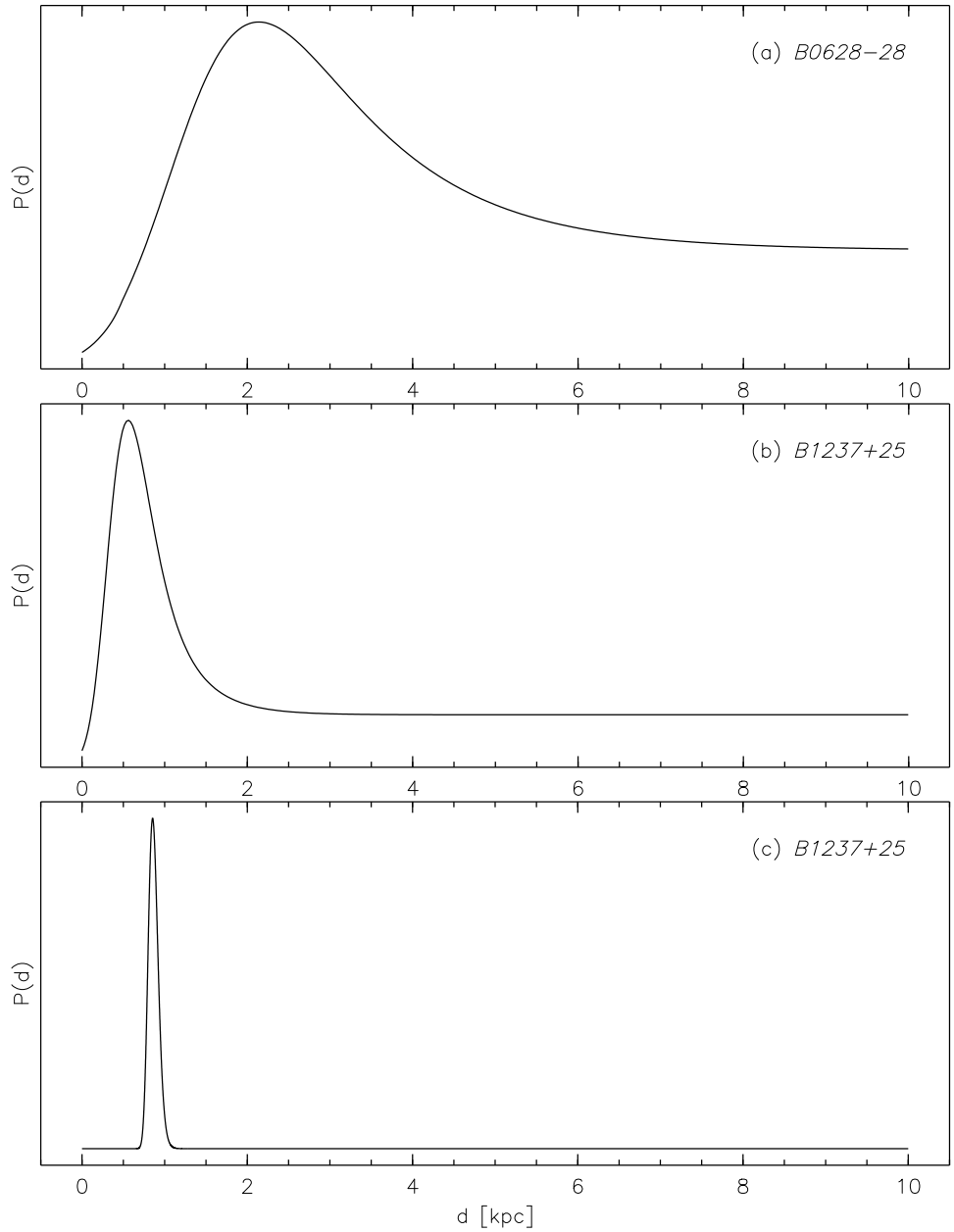

Fig. 1.— Examples of different distance PDFs, demonstrating their non-Gaussianity. The DM-derived distance PDFs for B0628-28 and B1237+25 are shown in panels (a) and (b) respectively. Note the finite probability density even at very large distances. The much more constraining PDF derived for B1237+25 from parallax is shown in panel (c). These PDFs are normalized so that their integral is 1.

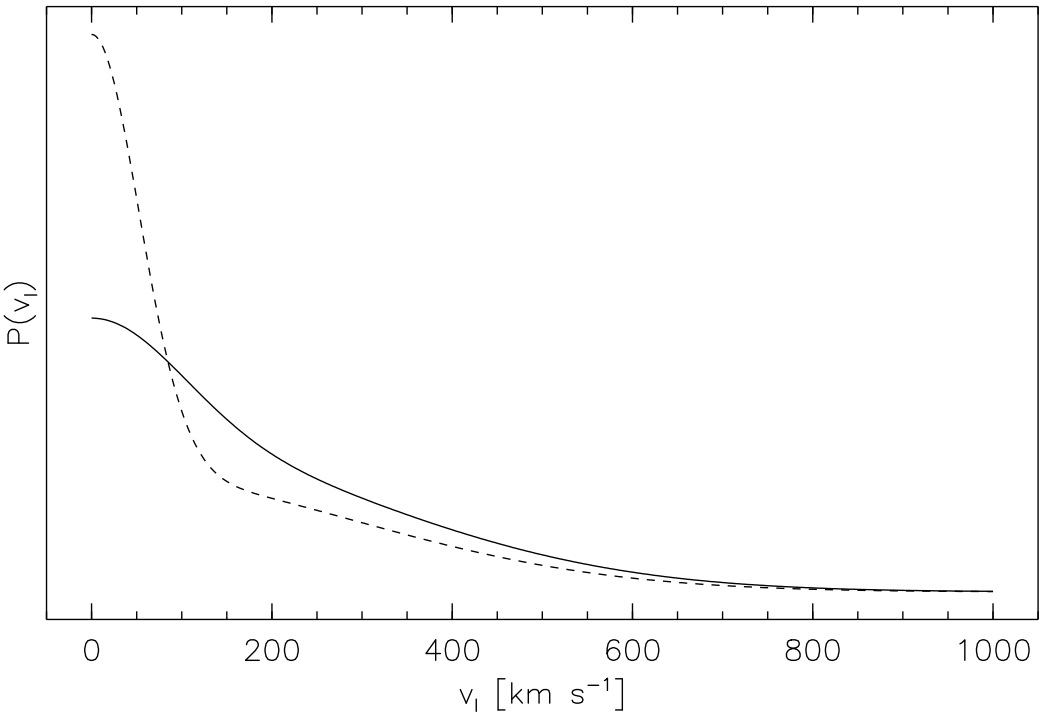

Fig. 2.— 1-dimensional best fit velocity PDFs from our proper motion study (solid) and from ACC (dashed).

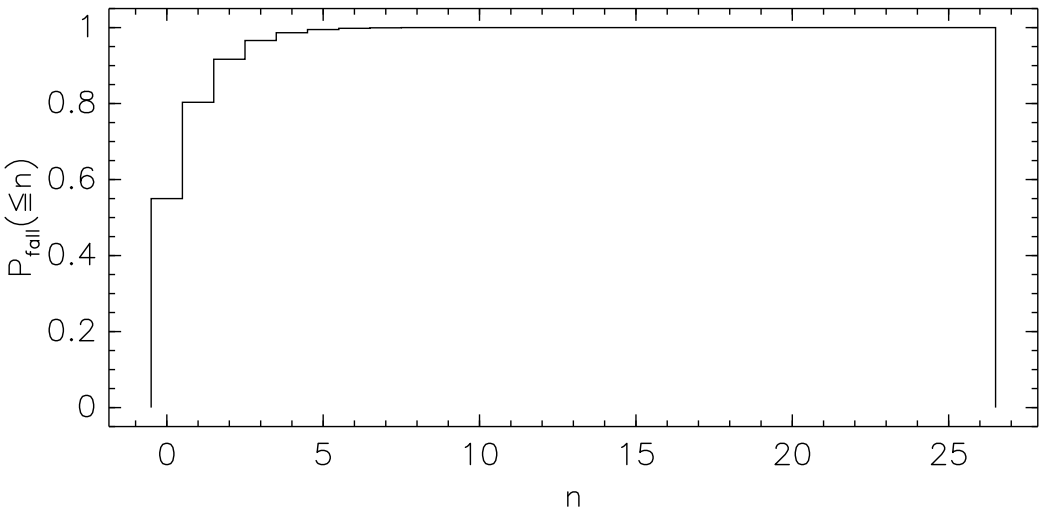

Fig. 3.— Cumulative probability distribution for the number of young ($\tau_{\rm char} < 20$ Myr) pulsars out of the 26 pulsar sample falling toward the plane.

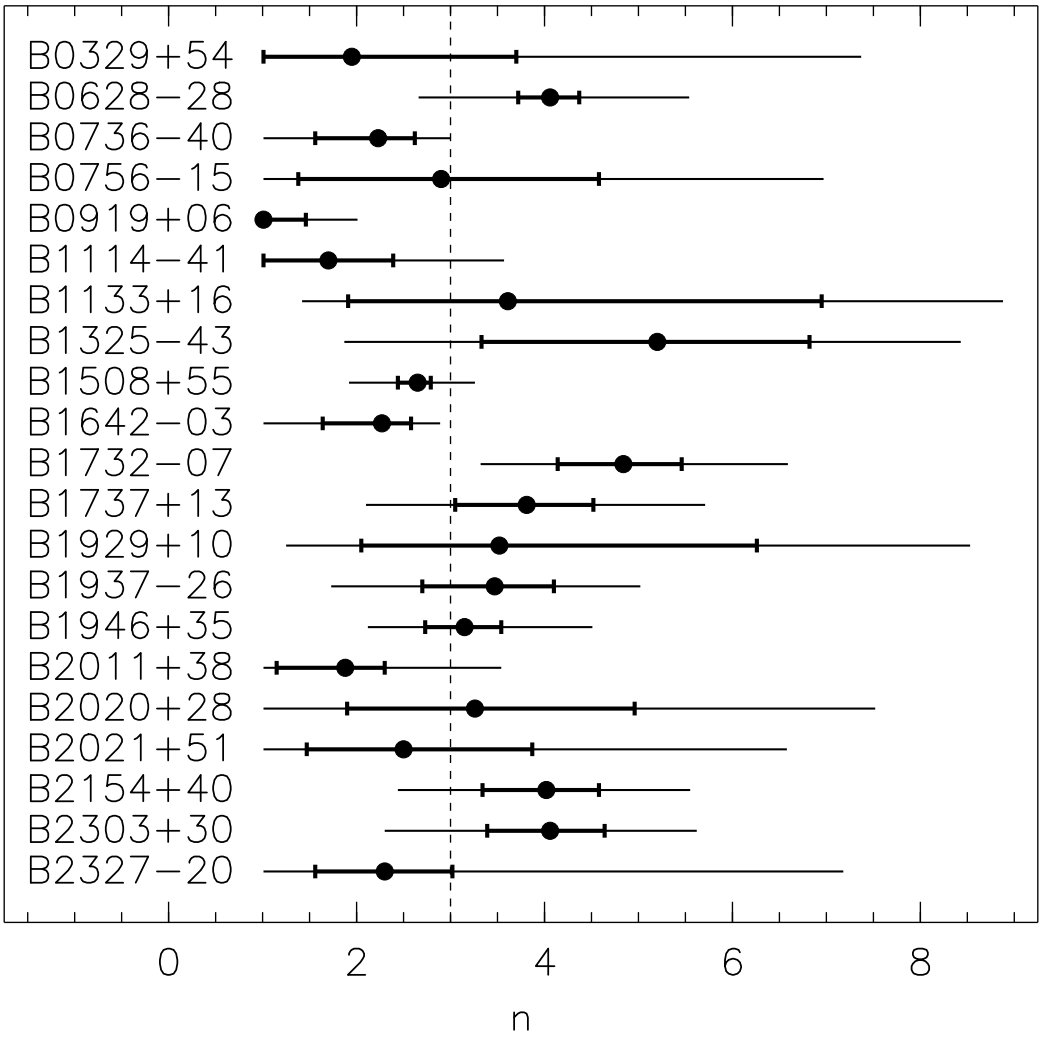

Fig. 4.— The braking indexes, n, for the 21 pulsars younger than 10 Myr. The most likely value of n for each pulsar is shown by a dot. The most compact 68% confidence intervals are denoted by the thick horizontal lines with vertical bars. The most compact 95% confidence intervals are denoted by the thin horizontal lines. The vertical dashed line indicates the nominal value of 3.

Table 1. Pulsars observed

Pulsar[1]	Observed Epochs[2]	Flux Density[3] (mJy)	Period (s)	$\tau_{\rm char}$ (Myr)	Number of Ref. Sources
B0011+47	94g 98bg 99g	5	1.241	34.9	21
B0149–16	86 92g 95g 99g	1.6	0.833	10.2	17
B0628–28	86 92 95 99	2	1.244	2.77	17
B0736–40	86 95 99	50	0.375	3.68	7
B0756–15	94g 98g 99g	0.8	0.682	6.69	10
B0835–41	94g 98 99	20	0.752	3.36	12
B0919+06	86 92g 95 98 99g	6	0.431	0.50	11
B1039–19	94g 98g 99g	1.4	1.386	23.3	5
B1114–41	92 95 99	3	0.943	1.88	4
B1237+25	92 95 98 99g	15	1.382	22.8	9
B1325–43	94g 98bg	2	0.533	2.80	9
B1508+55	92g 95 99g	8	0.740	2.34	14
B1534+12	94g 98bg 99	2	0.038	247	16
B1540–06	84 92g 94g 98bg 99	2	0.709	12.7	10
B1541+09	92 95 99	5.9	0.748	27.4	25
B1552–31	94g 99g	1.4	0.518	132	12
B1642–03	92 95 99	21	0.388	3.45	7
B1718–02	94g 99g	1	0.478	87.0	6
B1732–07	92g 99g	1.7	0.419	5.47	8
B1737+13	92g 99g	3.9	0.803	8.75	11
B1937–26	94 98 99g	3	0.403	6.68	7
B1943–29	92 99g	0.8	0.959	10.2	12
B1946+35	84 92 95 99	8.3	0.717	1.61	21
B2011+38	94 98 99	6.4	0.230	0.41	12
B2106+44	92g 99g 01	5.4	0.415	76.3	9
B2154+40	92g 95g 99	17	1.525	7.05	22
B2303+30	92g 95g 99g	2.2	1.576	8.62	11
B2327–20	94g 98bg 99	3	1.644	5.63	13

[1]Period, period derivative, and flux density are from the catalog of Taylor et al. (1995).

[2]last two digits of years of observation. Suffix ‘b’ indicates that some data from the A- to B-array reconfiguration was used. Suffix ‘g’ indicates pulsar gating.

[3]at 1400 MHz

Table 2. Measured parameters[a]

Pulsar	Right Asc.	Dec.	l	b	$\mu_\alpha \cos\delta$	μ_δ	Cov.	$\mu_l \cos b$	μ_b	Cov.
B0011+47	00:14:17.757	47:46:33.29	116.49	–14.63	19.3 ± 1.8	–19.7 ± 1.5	0.54	16.1 ± 1.9	–22.3 ± 1.4	0.48
B0149–16	01:52:10.858	–16:37:53.22	179.30	–72.45	3.1 ± 1.2	–27.2 ± 2.0	–0.12	23.0 ± 1.9	–14.8 ± 1.6	–0.47
B0628–28	06:30:49.433	–28:34:42.91	236.95	–16.75	–44.6 ± 0.9	19.5 ± 2.2	0.05	–34.9 ± 2.1	–33.9 ± 1.2	–0.57
B0736–40	07:38:32.329	–40:42:40.94	254.19	–9.19	–14.0 ± 1.2	12.8 ± 2.1	–0.54	–17.9 ± 2.2	–6.3 ± 1.0	–0.25
B0756–15	07:58:29.109	–15:28:09.78	234.46	7.22	1.2 ± 4.0	3.6 ± 5.6	–0.31	–2.4 ± 5.7	2.9 ± 3.7	–0.15
B0835–41	08:37:21.266	–41:35:15.05	260.90	–0.33	–2.3 ± 1.8	–17.8 ± 3.3	–0.59	12.8 ± 3.4	–12.6 ± 1.7	–0.48
B0919+06	09:22:14.008	06:38:22.70	225.42	36.39	18.8 ± 0.9	86.4 ± 0.7	0.05	–66.5 ± 0.8	58.4 ± 0.8	0.09
B1039–19	10:41:36.201	–19:42:13.44	265.59	33.59	–1.1 ± 2.6	14.4 ± 4.5	0.15	–9.2 ± 3.1	11.2 ± 4.2	–0.45
B1114–41	11:16:43.086	–41:22:43.96	284.45	18.06	–1.4 ± 4.8	7.1 ± 20.3	0.05	–3.9 ± 8.6	6.1 ± 19.0	–0.80
B1237+25	12:39:40.361	24:53:49.96	252.44	86.54	–104.5 ± 1.1	49.4 ± 1.4	0.05	–105.6 ± 1.2	–46.8 ± 1.3	–0.20
B1325–43	13:28:06.432	–43:57:44.12	309.87	18.41	3.3 ± 6.6	53.6 ± 22.6	0.18	11.3 ± 7.9	52.5 ± 22.2	0.54
B1508+55	15:09:25.646	55:31:32.53	91.32	52.28	–70.6 ± 1.6	–68.8 ± 1.2	0.22	–16.7 ± 1.2	97.2 ± 1.6	0.17
B1534+12	15:37:09.960	11:55:55.57	19.84	48.34	–7.6 ± 9.3	–31.6 ± 10.1	0.03	–31.5 ± 10.0	–7.9 ± 9.4	0.04
B1540–06	15:43:30.167	–06:20:45.42	0.56	36.60	–17.4 ± 2.4	–3.6 ± 2.7	0.42	–14.1 ± 3.0	10.8 ± 1.9	0.02
B1541+09	15:43:38.836	09:29:16.41	17.81	45.77	–7.3 ± 1.0	–4.0 ± 1.0	–0.12	–7.0 ± 1.0	4.4 ± 1.0	0.11
B1552–31	15:55:17.946	–31:34:20.16	342.69	16.75	60.6 ± 19.3	–77.3 ± 50.6	–0.37	–6.6 ± 31.5	–98.0 ± 44.0	0.75
B1642–03	16:45:02.051	–03:17:57.93	14.11	26.06	–3.7 ± 1.5	30.0 ± 1.6	0.53	23.3 ± 1.9	19.2 ± 1.1	–0.22
B1718–02	17:20:57.257	–02:12:24.15	20.13	18.93	–0.8 ± 3.7	–25.7 ± 4.5	0.18	–22.7 ± 4.7	–12.0 ± 3.6	0.08
B1732–07	17:35:04.965	–07:24:52.29	17.27	13.28	–2.4 ± 1.7	28.4 ± 2.5	0.01	23.3 ± 2.4	16.4 ± 2.0	0.31
B1737+13	17:40:07.332	13:11:56.64	37.08	21.67	–21.5 ± 2.2	–19.7 ± 2.2	–0.09	–26.7 ± 2.1	11.5 ± 2.3	0.06
B1937–26	19:41:00.405	–26:02:05.98	13.90	–21.82	12.1 ± 2.4	–9.9 ± 3.8	0.01	–5.0 ± 3.6	–14.8 ± 2.6	0.27
B1943–29	19:46:51.732	–29:13:47.03	11.10	–24.12	18.6 ± 8.9	–32.8 ± 20.3	–0.46	-25.1 ± 18.1	–28.2 ± 12.8	0.72
B1946+35	19:48:25.000	35:40:11.04	70.70	5.04	–12.6 ± 0.6	0.7 ± 0.6	–0.11	–6.4 ± 0.8	12.4 ± 0.9	0.12
B2011+38	20:13:10.355	38:45:43.17	75.93	2.47	–32.1 ± 1.7	–24.9 ± 2.3	–0.49	–38.5 ± 1.7	13.1 ± 2.3	0.47
B2106+44	21:08:20.481	44:41:48.81	86.90	–2.01	3.5 ± 1.3	1.4 ± 1.4	0.05	3.4 ± 1.4	–1.6 ± 1.3	0.07
B2154+40	21:57:01.844	40:17:45.99	90.48	–11.34	17.8 ± 0.8	2.8 ± 1.0	–0.77	15.6 ± 0.4	–9.0 ± 1.2	0.09
B2303+30	23:05:58.322	31:00:01.46	97.72	–26.65	1.5 ± 2.3	–20.0 ± 2.2	–0.14	–7.5 ± 2.1	–18.6 ± 2.3	–0.11
B2327–20	23:30:26.908	–20:05:29.92	49.39	–70.19	74.7 ± 1.9	5.3 ± 2.9	0.15	36.0 ± 2.8	–65.7 ± 1.9	0.23

[a]Positions are J2000.0 coordinates at epoch 1999.5, and are accurate to about 0.1 arcsecond. Proper motion measurements are in milliarcseconds per year. No corrections for differential galactic rotation have been made (see text).

Table 3. Comparisons with previous results

Pulsar	$\mu_\alpha \cos\delta$ mas yr^{-1}	μ_δ mas yr^{-1}	$\Delta\mu_\alpha$ σ	$\Delta\mu_\delta$ σ	reference
B0149–16	3.1 ± 1.2	–27.2 ± 2.0			
	35 ± 47	–75 ± 19	0.67	–2.51	1
B0628–28	–44.6 ± 0.9	19.5 ± 2.2			
	–37 ± 15	9 ± 7	0.50	–1.43	1
B0736–40	–14.0 ± 1.2	12.8 ± 2.1			
	–57 ± 7	–21 ± 11	–6.05	–3.02	1
B0919+06	18.8 ± 0.9	86.4 ± 0.7			
	18.35 ± 0.06	86.56 ± 0.12	–0.50	0.23	2
	13 ± 29	64 ± 37	–0.20	–0.61	3
B1237+25	–104.5 ± 1.1	49.4 ± 1.4			
	–106.82±0.17	49.92±0.18	–2.08	–0.37	4
	–106 ± 4	42 ± 3	–0.36	–2.23	5
B1508+55	–70.6 ± 1.6	–68.8 ± 1.2			
	–73 ± 4	–68 ± 3	–0.55	0.24	5
B1534+12	–7.6 ± 9.3	–31.6 ± 10.1			
	–1.5 ± 0.1	–25.6 ± 1.5	0.65	0.59	6
B1540–06	–17.4 ± 2.4	–3.6 ± 2.7			
	–11 ± 20	–1 ± 12	0.32	2.11	1
B1541+09	–7.3 ± 1.0	–4.0 ± 1.0			
	–12 ± 4	3 ± 3	–1.13	2.21	5
B1642–03	–3.7 ± 1.5	30.0 ± 1.6			
	41 ± 17	–25 ± 11	2.62	–4.95	5
B1718–02	–0.8 ± 3.7	–25.7 ± 4.5			
	26 ± 9	–13 ± 6	3.23	0.49	3
B1946+35	–13.9 ± 0.8	0.7 ± 0.9			
	–9 ± 7	–4 ± 8	0.88	–0.58	3
B2154+40	17.8 ± 0.8	2.8 ± 1.0			
	18 ± 1	–3 ± 1	0.16	–4.10	3
B2303+30	1.5 ± 2.3	–20.0 ± 2.2			
	13 ± 8	–33 ± 6	1.38	–2.03	5

Table 3—Continued

Pulsar	$\mu_\alpha \cos\delta$ mas yr^{-1}	μ_δ mas yr^{-1}	$\Delta\mu_\alpha$ σ	$\Delta\mu_\delta$ σ	reference

References. — (1) Fomalont et al. (1997) (2) Chatterjee et al. (2001) (3) Harrison et al. (1993) (4) Brisken et al. (2002) (5) Lyne et al. (1982) (6) Stairs et al. (1998)

Table 4. Properties of six pulsars from Brisken et al. (2002) used in the analysis

Pulsar	α_{J2000}	δ_{J2000}	μ_α (mas/yr)	μ_δ (mas/yr)	π (mas)	$\tau_{\rm char}$ (Myr)
B0329+54	$03^h32^m59^s.3862$	$54°34'43''.5051$	17.00 ± 0.27	-9.48 ± 0.37	0.94 ± 0.11	5.5
B0950+08	$09^h53^m09^s.3071$	$07°55'36''.1475$	-2.09 ± 0.08	29.46 ± 0.07	3.82 ± 0.07	17.5
B1133+16	$11^h36^m03^s.1829$	$15°51'09''.7257$	-73.95 ± 0.38	368.05 ± 0.28	2.80 ± 0.16	5.0
B1929+10	$19^h32^m13^s.9496$	$10°59'32''.4178$	94.82 ± 0.26	43.04 ± 0.15	3.02 ± 0.09	3.1
B2020+28	$20^h22^m37^s.0718$	$28°54'23''.0300$	-4.38 ± 0.53	-23.59 ± 0.26	0.37 ± 0.12	2.9
B2021+51	$20^h22^m49^s.8655$	$51°54'50''.3881$	-5.23 ± 0.17	11.54 ± 0.28	0.50 ± 0.07	2.7

Table 5. Braking index measurements to date

Pulsar	n	Reference
B0531+21 (Crab)	2.51 ± 0.01	Lyne et al. 1993
B0540−69	2.04 ± 0.02	Gouiffes et al. 1992
B0833−45 (Vela)	1.4 ± 0.2	Lyne et al. 1996
B1046−58	2.1 ± 0.2	Urama 2002
J1119−6127	2.91 ± 0.05	Camilo et al. 2000
B1509−58	2.837 ± 0.001	Kaspi et al. 1994